The Canadian Mineralogist
Vol. 51, pp. 851-860 (2013)
DOI: 10.3749/canmin.51.6.851

SINNERITE, $Cu_6As_4S_9$, FROM THE LENGENBACH QUARRY, BINN VALLEY, SWITZERLAND: DESCRIPTION AND RE-INVESTIGATION OF THE CRYSTAL STRUCTURE

LUCA BINDI[§]

Dipartimento di Scienze della Terra, Università degli Studi di Firenze, Via G. La Pira 4, I-50121 Firenze, Italy and CNR – Istituto di Geoscienze e Georisorse, Sezione di Firenze, Via G. La Pira 4, I-50121 Firenze, Italy

EMIL MAKOVICKY

Department of Geoscience and Resource Management, University of Copenhagen, Østervoldgade 10, 1350 Copenhagen, Denmark

FABRIZIO NESTOLA

Dipartimento di Geoscienze, Università degli Studi di Padova, Via Gradenigo 6, I-35131 Padova, Italy

LUCA DE BATTISTI

FGL (Forschungsgemeinschaft Lengenbach), Via dello Storno 18, I-20147 Milano, Italy

ABSTRACT

We have characterized the crystal structure of sinnerite, $Cu_6As_4S_9$, a rare sulfosalt mineral from the ores of the Lengenbach quarry, Binn Valley, Canton Valais, Switzerland, by single-crystal X-ray diffraction and chemical analysis. We found sinnerite to be structurally identical to synthetic $Cu_6As_4S_9$. It is triclinic, space group $P\bar{1}$, with cell parameters: a 9.103(2), b 9.860(3), c 9.111(2) Å, α 90.27(2), β 109.53(2), γ 107.58(2)°, V 729.6(4) Å^3, and $Z = 2$. Semi-quantitative SEM-EDS analyses confirmed the $Cu_6As_4S_9$ stoichiometry. The crystal structure of an untwinned crystal has been refined to $R_1 = 5.45\%$. It consists of a sphalerite substructure with 2/5 of the tetrahedra replaced by AsS_3 pyramids; four pyramids form As_4S_{12} clusters around the vacant anion positions of the sphalerite archetype. These pyramids are linked into twisted and branched chain-like structures with compositions As_3S_7 and As_5S_{11}. The chains are linked by CuS_4 tetrahedra. Packing of these chains results in the OD (order-disorder) character of the sinnerite structure.

Keywords: sinnerite, crystal structure, sulfosalts, Lengenbach, Switzerland

INTRODUCTION

The Lengenbach quarry, located in the Binn Valley, Canton Valais, Switzerland, is one of the premium localities for sulfosalt minerals, including Pb-sulfosalts (*e.g.*, sartorite, baumhauerite, rathite, liveingite, dufrénoysite, jordanite), Pb-Tl-sulfosalts (*e.g.*, hutchinsonite, hatchite, wallisite, dalnegroite), Pb-Ag-Cu-sulfosalts (*e.g.*, marrite, seligmannite, lengenbachite), and Tl-sulfosalts (*e.g.*, lorandite, imhofite, raberite, philrothite). Copper- (*e.g.*, binnite, sinnerite, nowackiite) and Ag-sulfosalts (*e.g.*, stephanite, pyrargyrite, proustite, xanthoconite) are more rare but present. Among these minerals, sinnerite was identified as a new mineral species by Marumo & Nowacki (1964), who studied ore minerals occurring on the Lengenbach dolomite. Preliminary X-ray investigations of the mineral pointed out a complicated superlattice structure pattern with a small subcell. The reported dimensions for the subcell were: a 3.72(1), b 3.70(1), c 5.24(1) Å, and $\alpha = \beta = \gamma = 90°$. Later, Makovicky & Skinner (1972) were able to solve the composition and symmetry of sinnerite using the material synthesized by Maske & Skinner (1971) during their study of the Cu–As–S system. Despite the

§ *Corresponding author e-mail address*: luca.bindi@unifi.it

presence of an extremely pronounced sphalerite-like substructure with $a \sim 5.25$ Å, Makovicky & Skinner (1972) demonstrated the triclinic nature of sinnerite and concluded that both natural and synthetic crystals are complexly twinned (by reticular pseudo-merohedry). Later, the same authors (Makovicky & Skinner 1975) were able to propose a structural model for the synthetic analogue of sinnerite and showed that the twinning in such a compound produces twin aggregates containing 24 individuals and simulates a $\bar{4}3m$ cubic symmetry. Due to the pervasive twinning and to the very low number of collectable X-ray reflections (607 reflections, Rw = 17.2%) from a six-fold twin, the atom coordinates and the bond distances given by Makovicky & Skinner (1975) showed large errors. Moreover, a crystal-structure refinement of the natural material was not done at that time.

To help resolve the details of the structure of sinnerite, here we present new structural data from a gem-quality, untwinned sinnerite crystal recovered from a specimen originating from the Lengenbach quarry, Binn Valley, Switzerland.

Occurrence, Composition, and X-Ray Crystallography

Sinnerite was found in a rock-sample from the realgar-rich zone (the so-called zone 1; Graeser *et al.* 2008) collected in 1998. It occurs as very rare elongated crystals grown on realgar and is closely associated with coloradoite, described for the first time for the Lengenbach quarry (Fig. 1). Sinnerite exhibits a subhedral to anhedral grain morphology, and does not show any inclusions of, or intergrowths with, other minerals. The maximum grain size of sinnerite is about 150 μm.

A chemical analysis using energy dispersive spectrometry was performed using a SEM JEOL-5610 LV. The crystal fragment was found to be homogeneous within analytical error and the $Cu_6As_4S_9$ stoichiometry was confirmed (Cu 39.3, As 30.9, and S 29.8 wt.% of elements).

A crystal fragment (100 × 115 × 130 μm) was selected for the X-ray single-crystal diffraction study that was done with a STOE-STADI IV CCD single-crystal diffractometer (Table 1). No systematic absences were observed in the collected data set, thus leading to the choice of the space groups $P1$ and $P\bar{1}$. The statistical tests on the distribution of $|E|$ values ($|E^2 - 1| = 0.745$) did not indicate the presence of an inversion center, thus suggesting the choice of the space group $P1$. Detectable traces of twinning were absent. The positions of most of the atoms (Cu, As, and some S atoms) were determined by means of direct methods (Sheldrick 2008). A least-squares refinement on F^2 using these heavy-atom positions produced an R factor of 0.135. Three-dimensional difference Fourier synthesis yielded the position of the remaining sulfur atoms. The SHELXL program (Sheldrick 2008) was used for the refinement of the structure. The occupancy of all the sites was left free to vary (Cu *versus* vacancy; As *versus* vacancy; S *versus* vacancy) and all refined to full occupancy. Neutral scattering curves for Cu, As, and S were taken from the *International Tables for X-ray Crystallography* (Ibers & Hamilton 1974). At the final stage, with isotropic atomic displacement parameters for all atoms and no constraints, the residual value settled at $R = 0.0545$ for 1028 observed reflections [$2\sigma(I)$ level] and 153 parameters and at $R = 0.0567$ for all 3456 independent reflections. Experimental details and R indices are given in Table 1. Fractional atomic coordinates and isotropic displacement parameters are reported in Table 2. Bond distances are given in Table 3. A list of the observed and calculated structure factors is available from the Depository of Unpublished Data, MAC website [document Sinnerite CM51_851].

Results and Discussion

Crystal structure – a dual description

The crystal structure of sinnerite is a close homeotype of the zincblende (sphalerite) structure, as revealed by the strong reflections of a pseudocubic subcell (Makovicky & Skinner 1972). The strongest contributions to the true-cell reflections result from the presence

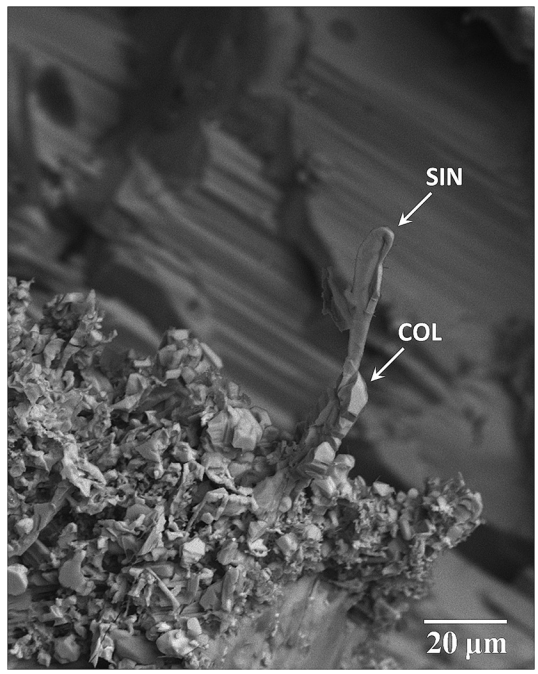

Fig. 1. Sinnerite (SIN) on realgar associated with coloradoite (COL).

of sulfur vacancies in the centers of two crystallographically independent As_4S_{12} clusters and from the deviation of As sites from the regular tetrahedral arrangement.

The structure of sinnerite contains eight different AsS_3 coordination pyramids and 12 distinct CuS_4 coordination tetrahedra (Fig. 2). There are 18 distinct S positions in these polyhedra. Two groups of four AsS_3 pyramids form two crystallographically distinct As_4S_{12} clusters, with As barycentres at (0.18610, 0.04947, 0.18190) (Fig. 3) and (0.53835, 0.64395, 0.63825) in terms of sinnerite lattice, and with individual AsS_3 pyramids in clusters separated from one another. The majority of pyramids have average As–S bond lengths in the range 2.26–2.31 Å, but As6 has an average As–S bond length equal to 2.423 Å, whereas As3 shows 2.217 Å, followed by As5 with 2.227 Å. These deviations are accompanied by deviations of calculated bond-valence values from the bulk of As atoms. The sulfurs S7 and S11, bonded to As6, have elevated displacement parameters (Table 2), as does As7, whereas S2 and S15, attached to As5, and S3, attached to As6, display higher bond-valence values. Placement of these atoms in the structure and possible reasons for these deviations from the average values will be discussed below.

TABLE 1. CRYSTALLOGRAPHIC DATA AND REFINEMENT PARAMETERS FOR SINNERITE

Crystal data	
Ideal formula	$Cu_6As_4S_9$
Crystal system	triclinic
Space group	*P*1
Unit-cell parameters (Å, °)	9.103(2) 9.860(3) 9.111(2) 90.27(2) 109.53(2) 107.58(2)
Unit-cell volume (Å^3)	729.6(4)
Z	2
Crystal size (mm)	0.100 × 0.115 × 0.130
Data collection	
Diffractometer	STOE-STADI IV CCD
Temperature (K)	298(3)
Radiation, wavelength (Å)	Mo*K*α, 0.71073
$2\theta_{max}$ for data collection (º)	58.02
Crystal-detector dist. (mm)	60
h, *k*, *l* ranges	–9 to 12, –12 to 12, –12 to 9
Axis, frames, width (º), time per frame (s)	ω, 435, 1.00, 40
Total reflections collected	7725
Unique reflections (R_{int})	3845 (0.081)
Unique reflections $I > 2\sigma(I)$	1028
Data completeness to θ_{max} (%)	99.7
Absorption correction method	X-RED and X-SHAPE
Structure refinement	
Refinement method	Full-matrix least-squares on F^2
Data/restraints/parameters	1028/3/154
R_1 [$I > 2\sigma(I)$], wR_2 [$I > 2\sigma(I)$]	0.0545, 0.0555
R_1 all, wR_2 all	0.0567, 0.0612
Goodness-of-fit on F^2	1.042
Largest diff. peak and hole (e$^-$/Å^3)	0.98, –0.78

$R_{int} = (n/n - 1)^{1/2} [F_0^2 - F_0(mean)^2] / \sum F_0^2$
$R_1 = \sum || F_0 | - | F_c || / \sum | F_0 |$
$wR_2\{\sum[w(F_0^2 - F_0^2] / \sum [w(F_0^2)^2]\}^{1/2}$
$GooF = \{\sum[2(F_0^2 - F_c^2)^2] / (n - p)\}^{1/2}$ Where *n* = no. of reflections, *p* = no. of refined parameters

The average of bond-valence values (calculated from the curves of Brese & O'Keeffe 1991) for As is 2.945 *bvu*, but those for Cu (1.372 *bvu*) and S (2.223 *bvu*) are higher than expected (Table 4). Cu1 and Cu9 have elevated displacement parameters; these can tentatively be explained by their bonds to S atoms bonded to the aforementioned As atoms with elevated displacement parameters and/or deviating bond characteristics.

An alternative description of the crystal structure of sinnerite, in terms of chains of short As–S bonds (Makovicky & Skinner 1975), discerns two types of chains: twisted branched chains with compositions As_3S_7 and As_5S_{11} (Fig. 4). The longer chain is an extended version of the shorter one. The chains are 'immersed' in an environment of CuS_4 tetrahedra of the zincblende-like structure. The first type of As_4S_{12} cluster combines As2 and As3 from the As_3S_7 chain and As1 and As4 from the As_5S_{11} chain. The As–As distances vary between 3.36 and 3.62 Å, the distances of As atoms to their barycenter are 2.07–2.23 Å, and S–S distances in the periphery of the cluster are in the range of 3.37–3.89 Å. The second type of As_4S_{12} cluster combines As8 from the As_3S_7 chain with three arsenic atoms (As5, 6, and 7) from the As_5S_{11} chain. This cluster appears larger, with As–As distances from 3.48 to 3.71 Å (the longest distance occurs between As8 and As6), As-to-barycenter distances from 2.14 to 2.26 Å, and S–S distances from 3.37 to 3.89 Å. Both As_4S_{12} clusters share S–S edges with three adjacent clusters and are arranged in $(10\bar{1})$ planes of the sinnerite structure, being separated by As–free interspaces. The relationship between clusters (represented as cubo-octahedra defined by peripheral S atoms) is illustrated in Figure 5, in which relevant fragments of As–S chains are also included.

OD phenomena

The OD phenomena are best described by the arrangement of the twisted branched As_3S_7 and As_5S_{11} chains, whereas the CuS_4 tetrahedra enveloping them can be considered a 'passive' geometrical element. An alternative description of these phenomena, in terms of contact and attachment schemes for the two types of As_4S_{12} clusters present in the sinnerite structure, is given in Makovicky & Skinner (1975).

The two types of branched chains are arranged as alternating As_3S_7 and As_5S_{11} layers parallel to (010) of the sinnerite lattice (Fig. 6). Although not obvious in the views along [100] or [001], the As_3S_7 chains are distributed in their layer in a highly symmetrical *cm*

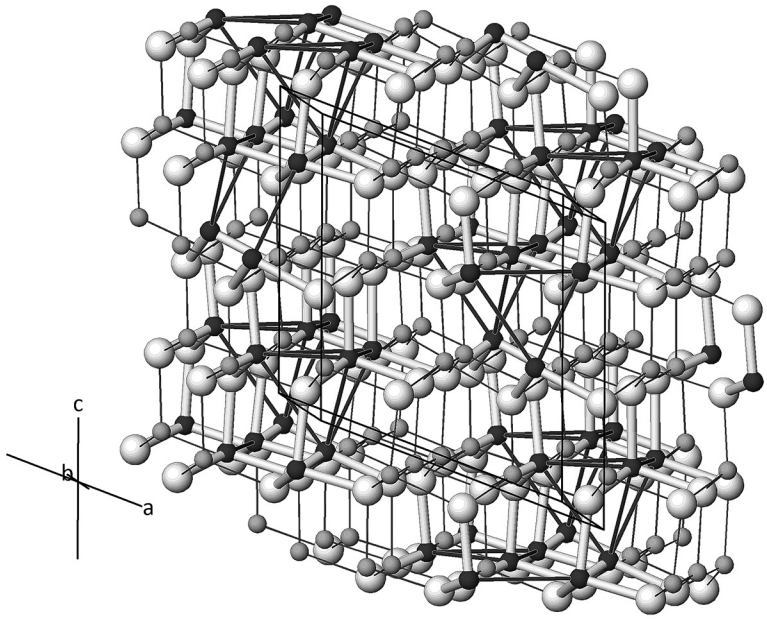

FIG. 2. The crystal structure of sinnerite. As: black spheres, Cu: grey spheres, S: larger white spheres. Short As–S bonds are rendered in white, and the tetrahedral Cu–S bonds as thin lines. The thick black lines are As–As joins, too long for any bonding interactions, and are used here to delineate the inner volumes of tetrahedral As_4 clusters.

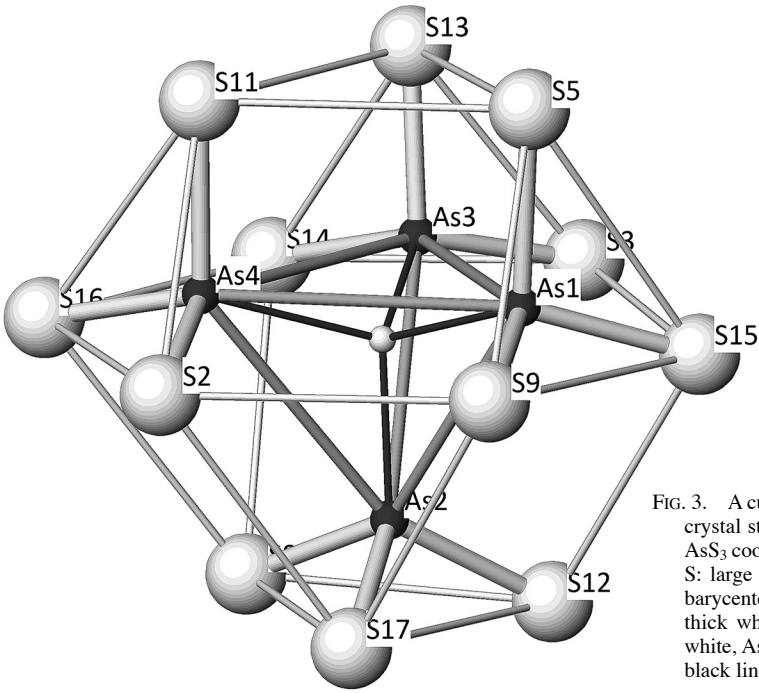

FIG. 3. A cubo-octahedral As_4S_{12} cluster from the crystal structure of sinnerite composed of four AsS_3 coordination pyramids. As: black spheres, S: large white spheres. A small white sphere: barycenter of the As_4 cluster. Short As–S bonds: thick white sticks, schematic S–S joins: thin white, As–As joins: grey, Barycentre–As joins: black lines.

FIG. 4. The As_5S_{11} (left, dark bonds) and As_3S_7 (right, light bonds) chains from the crystal structure of sinnerite.

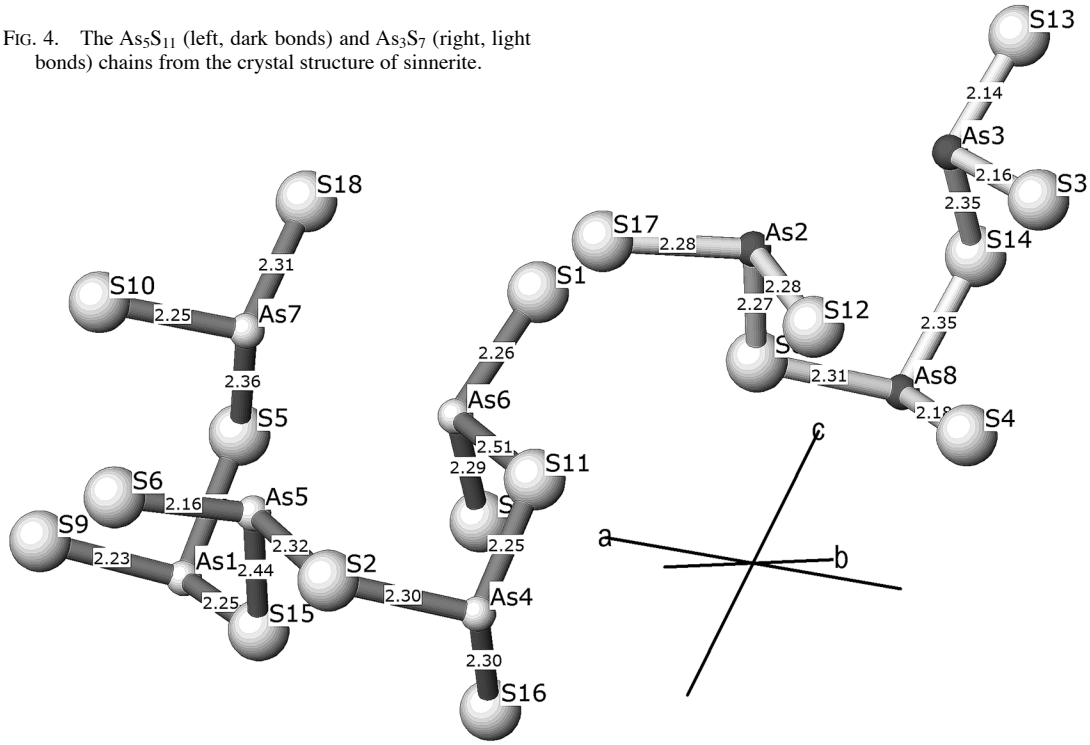

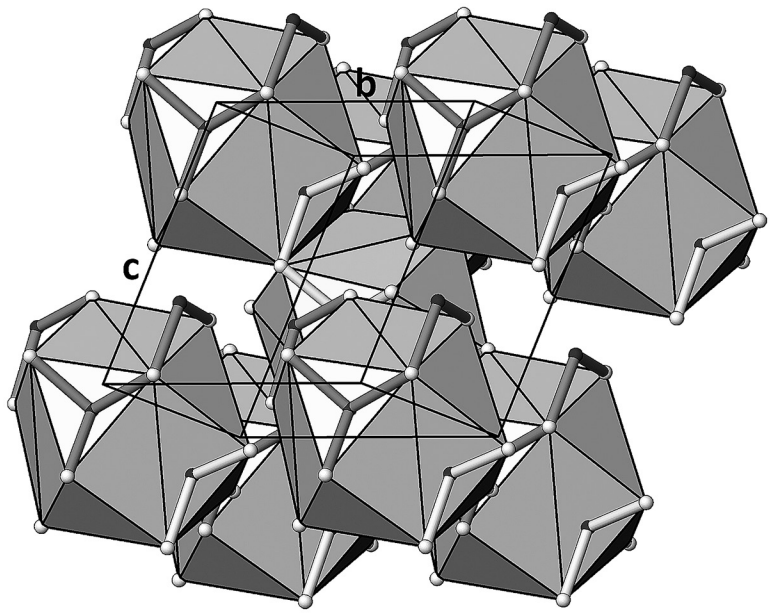

FIG. 5. The arrangement of As_4S_{12} clusters (opaque cubo-octahedra) in the crystal structure of sinnerite. The $(10\bar{1})$ planes of the sinnerite structure, occupied by the clusters, and separated by As-free interspaces, are inclined in the figure, running from the upper left corner towards the right lower corner. Portions of As–S chains have the same coloring as in Figure 4.

TABLE 2. ATOM COORDINATES (Å) AND ISOTROPIC ATOMIC DISPLACEMENT PARAMETERS (Å^2) FOR SINNERITE

atom	*x*/*a*	*y*/*b*	*z*/*c*	U_{iso}
As1	0.376(2)	0.234(1)	0.326(2)	0.019(5)
As2	0.192(1)	0.057(1)	–0.036(1)	0.010(4)
As3	0.959(1)	0.062(1)	0.188(1)	0.013(3)
As4	0.225(2)	0.845(1)	0.275(2)	0.021(4)
As5	0.534(2)	0.641(1)	0.394(2)	0.027(5)
As6	0.291(1)	0.626(1)	0.638(1)	0.010(3)
As7	0.589(2)	0.462(2)	0.734(2)	0.037(5)
As8	0.737(2)	0.849(2)	0.790(2)	0.024(4)
Cu1	0.777(2)	0.644(2)	0.130(2)	0.036(6)
Cu2	0.340(2)	0.450(2)	–0.010(2)	0.023(5)
Cu3	0.471(2)	0.840(2)	0.027(2)	0.014(4)
Cu4	0.022(2)	0.649(2)	0.880(2)	0.029(6)
Cu5	0.975(2)	0.845(1)	0.517(2)	0.016(4)
Cu6	0.827(2)	0.460(2)	0.490(2)	0.023(5)
Cu7	0.137(2)	0.245(2)	0.571(2)	0.025(5)
Cu8	0.898(1)	0.244(1)	0.862(1)	0.020(4)
Cu9	0.681(2)	0.041(2)	0.437(2)	0.036(7)
Cu10	0.440(2)	0.047(2)	0.689(2)	0.022(5)
Cu11	0.624(2)	0.242(2)	0.097(2)	0.029(5)
Cu12	0.075(2)	0.434(2)	0.225(2)	0.024(5)
S1	0.276(3)	0.655(3)	0.886(3)	0.016(8)
S2	0.478(3)	0.832(3)	0.301(3)	0.014(8)
S3	0.884(3)	0.244(2)	0.107(3)	0.015(6)
S4	0.707(2)	0.047(2)	0.691(2)	0.018(6)
S5	0.405(3)	0.247(2)	0.598(3)	0.021(6)
S6	0.769(3)	0.652(2)	0.376(3)	0.023(6)
S7	0.061(4)	0.432(3)	0.471(3)	0.037(8)
S8	–0.002(3)	0.865(3)	0.791(3)	0.014(8)
S9	0.621(3)	0.226(2)	0.332(3)	0.017(7)
S10	0.836(3)	0.451(2)	0.741(3)	0.027(7)
S11	0.232(4)	0.845(3)	0.519(4)	0.035(8)
S12	0.134(3)	0.241(3)	0.814(3)	0.016(8)
S13	0.932(3)	0.043(2)	0.412(3)	0.014(7)
S14	0.733(3)	0.868(2)	0.035(3)	0.019(6)
S15	0.326(3)	0.441(3)	0.242(4)	0.018(8)
S16	0.017(3)	0.638(3)	0.132(4)	0.021(7)
S17	0.428(3)	0.051(3)	0.948(3)	0.018(7)
S18	0.585(3)	0.434(3)	–0.011(3)	0.020(6)

scheme, with deviations from this symmetry equal only to a fraction of one Å. All As_3S_7 chains point in the same direction along the short diagonal of the (010) face (Figs. 7 and 8). The As_3S_7 layer is also polar in the [010] direction, with the 'front side' containing protruding S atoms and 'back side' with near-horizontal As–S bonds (Fig. 6). The As_5S_{11} chains form a polar layer of their own, pointing again along one direction of the short diagonal of the (010) face but their asymmetric attachment (Figs. 7 and 8) reduces the layer symmetry to *p*1 or, in order to keep the interlayer match simple, to *c*1, which has the same mesh axes as those selected for the As_3S_7 layer. Again, the 'top' and the 'bottom' of the As_5S_{11} layer are different. The 'front side' of it, with protruding S atoms, contains an additional group of two As polyhedra and the 'front' sides of the two layer types face one another, as also do the 'back' sides of them (Fig. 6).

When choosing the 'central' As atoms of the two groups (As8 for As_3S_7 and As4 for As_5S_{11}) as arbitrary origins, in the 'front-to-front' contact of the layers the As4 atom lies above the As3 atom of the As_3S_7 group. Because of the extreme regularity of the As_3S_7 layer, it could equally well lie above the opposing, As2, atom, but the As_5S_{11} group must then be an enantiomorph (chiral edition, a mirror image) of the group depicted in Figure 7. There is a sideways shift between the origins of the two layer types, defined by the As8 and As4 atoms, respectively, which is equal to $0.09\,\boldsymbol{a} + 0.34\,\boldsymbol{c}$ in

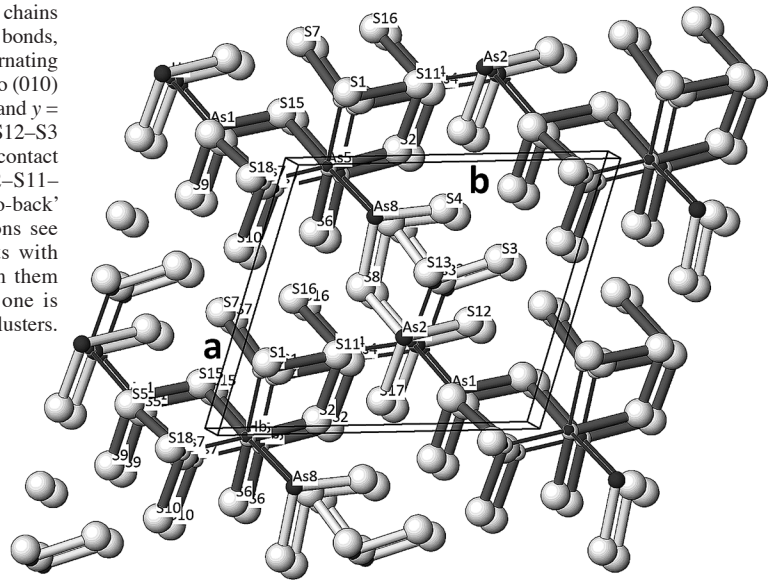

FIG. 6. The two types of branched chains (indicated by light and dark As–S bonds, respectively) are arranged as alternating As_3S_7 and As_5S_{11} layers parallel to (010) of the sinnerite lattice, at $y = 0.5$ and $y = 0.0$, respectively. The S9–As1–S12–S3 line defines the 'front-to-front' contact of the two layer types; the S2–S11–S8–As8 line defines the 'back-to-back' contact of them (for implications see text and Figs. 7–8). Black dots with three black lines radiating from them towards As atoms (the fourth one is vertical) are barycentres of As_4 clusters.

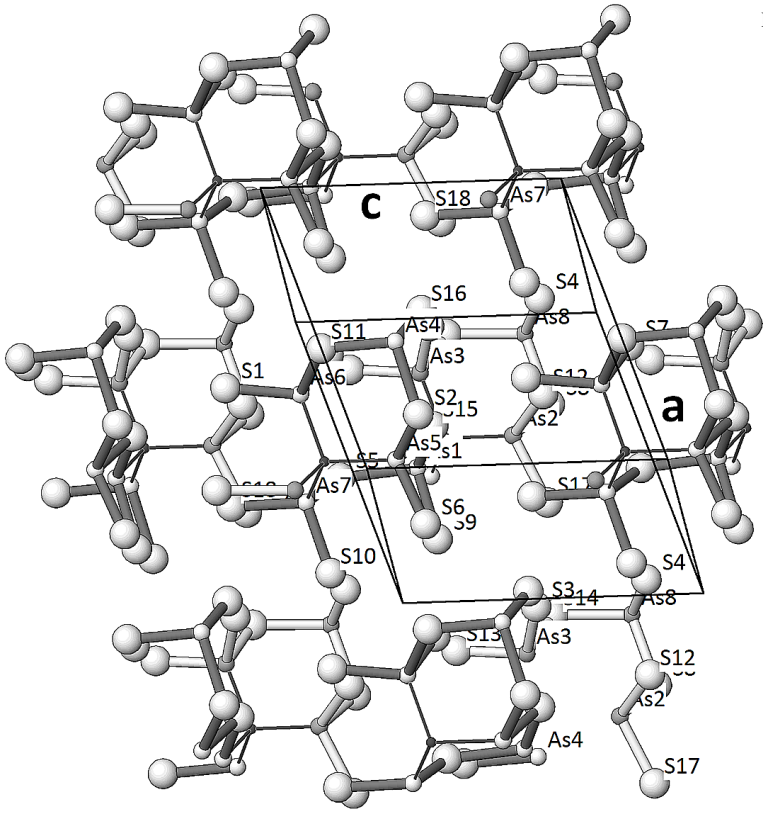

FIG. 7. A pair of As_3S_7 and As_5S_{11} layers parallel to (010) of the sinnerite lattice in a front-to-front contact. A slightly inclined projection on (010). The As_3S_7 chains have light-colored As–S bonds, the As_5S_{11} chains have dark colored bonds. Black dots are barycentres of As_4 clusters, with barycentre–As joins illustrated as black lines. Copper coordination tetrahedra (not illustrated) fill the remaining spaces. The OD potential of this layer pair is outlined in the text.

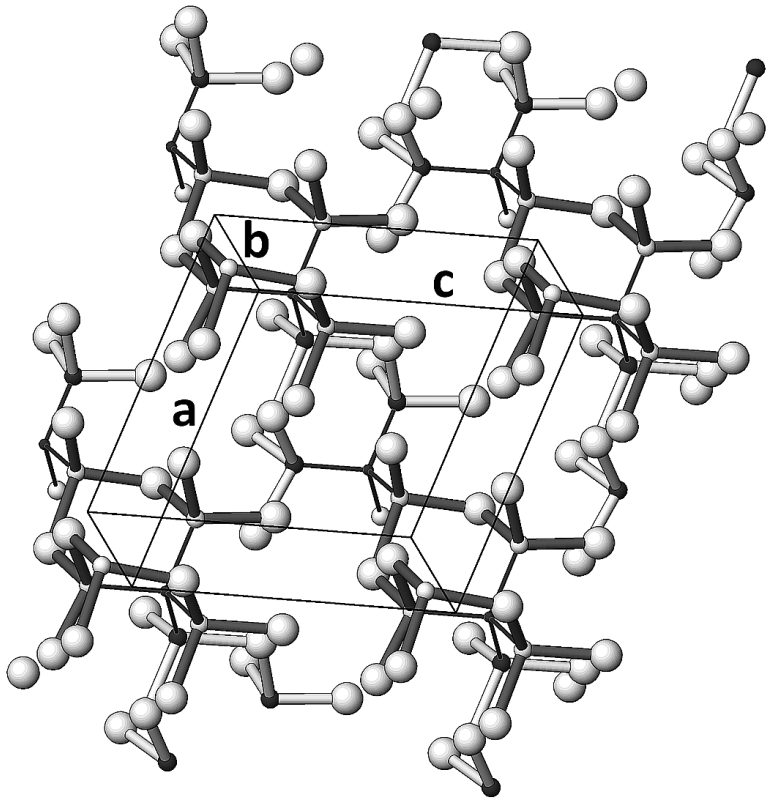

FIG. 8. A pair of As_3S_7 and As_5S_{11} layers parallel to (010) of the sinnerite lattice in a back-to-back contact. For conventions and comments see Figure 7.

terms of sinnerite axes (in the projection along [010]*, not along [010]).

With the same choice of layer origins, the 'back-to-back' fit of the two layer types forms a pair where the As4 atom (and the As_5S_{11} group) is shifted from the coincidence with the As8 atom by ½ of the short face diagonal of (010) in such a way that the terminal As7 atom of the 'branch' of the As_5S_{11} group overlaps the 'origin' (*i.e.*, the As8 atom) of the As_3S_7 group (Fig. 8). The origin of the As_5S_{11} layer, fixed on As4, is displaced from the origin of the As_3S_7 layer (the As8 atom) by $0.49\boldsymbol{a} + 0.48\boldsymbol{c}$ of the sinnerite lattice (in projection along [010]* of the sinnerite lattice). This symmetrical disposition is desymmetrized by the one-sided branching of the As_5S_{11} group, and within this layer pair there is an equal probability of attachment of the As_5S_{11} group as drawn in Figure 8 or of attachment of its enantiomorph (mirror image), which will have the additional As1–As7 branch situated on its opposite arm. In both described cases, attachment of the enantiomorph groups results in exchange of the *a* and *c* axes of the unit cell.

To summarize, sinnerite is an OD structure composed of two kinds of polar layers, with plane groups *cm* and *p*1 (conveniently described as *c*1), respectively, which allow alternative choices of layer stacking according to which enantiomorph of the *p*1 structure is present. This choice takes place at every layer contact and proceeds differently on the opposite surfaces of the thinner, As_3S_7 layer. According to Makovicky & Skinner (1975), a twin law resulting from one occurrence of the enantiomorph attachment is $m \,||\, (\bar{4}\,\bar{1}4)$ of the sinnerite lattice.

Slicing the two types of layers and their contact into individual (010) atomic planes reveals the extreme underlying regularity and local *cm* plane-group symmetry of this *P*1 structure. Atom configurations in the (010) planes through the cores of the As_3S_7 and As_5S_{11} groups are identical: bonded As–S groups paired around the imaginary barycenter of the As_4 cluster, aligned parallel to the long diagonal of the (010) face, and interspaced by one intermediate S atom. We observe an overall *cm* pattern. The back-to-back boundary of the two layer kinds, mentioned above, is unique, with kinked S–As–S groups arranged in a *cm* pattern,

TABLE 3. SELECTED BOND DISTANCES (Å) FOR SINNERITE

As1—S9	2.24(3)	Cu4—S10	2.20(3)
As1—S15	2.30(3)	Cu4—S1	2.28(3)
As1—S5	2.40(3)	Cu4—S16	2.31(3)
		Cu4—S8	2.32(3)
As2—S17	2.22(3)		
As2—S8	2.29(3)	Cu5—S6	2.24(3)
As2—S12	2.35(3)	Cu5—S13	2.26(3)
		Cu5—S11	2.34(3)
As3—S13	2.14(3)	Cu5—S8	2.44(3)
As3—S3	2.16(2)		
As3—S14	2.35(2)	Cu6—S10	2.26(3)
		Cu6—S6	2.28(3)
As4—S11	2.21(3)	Cu6—S7	2.29(4)
As4—S2	2.28(3)	Cu6—S9	2.54(3)
As4—S16	2.33(3)		
		Cu7—S7	2.25(4)
As5—S6	2.17(3)	Cu7—S12	2.23(3)
As5—S2	2.20(3)	Cu7—S13	2.34(3)
As5—S15	2.31(3)	Cu7—S5	2.36(3)
As6—S1	2.33(3)	Cu8—S3	2.28(3)
As6—S7	2.40(3)	Cu8—S4	2.31(2)
As6—S11	2.54(3)	Cu8—S12	2.34(3)
		Cu8—S10	2.45(3)
As7—S10	2.27(3)		
As7—S5	2.30(3)	Cu9—S9	2.20(3)
As7—S18	2.36(3)	Cu9—S4	2.24(3)
		Cu9—S2	2.31(3)
As8—S4	2.20(3)	Cu9—S13	2.36(3)
As8—S14	2.25(3)		
As8—S8	2.34(3)	Cu10—S5	2.22(3)
		Cu10—S11	2.38(3)
Cu1—S16	2.20(3)	Cu10—S4	2.42(3)
Cu1—S6	2.27(3)	Cu10—S17	2.40(3)
Cu1—S18	2.30(3)		
Cu1—S14	2.47(3)	Cu11—S9	2.16(3)
		Cu11—S18	2.20(3)
Cu2—S18	2.29(3)	Cu11—S17	2.21(3)
Cu2—S15	2.34(3)	Cu11—S3	2.33(3)
Cu2—S1	2.39(3)		
Cu2—S12	2.44(3)	Cu12—S3	2.11(3)
		Cu12—S15	2.22(3)
Cu3—S1	2.15(3)	Cu12—S7	2.28(3)
Cu3—S14	2.30(3)	Cu12—S16	2.33(3)
Cu3—S17	2.31(3)		
Cu3—S2	2.47(3)		

although they alternatively come from the groups to the left and to the right of the boundary, *i.e.*, they are *pm* in (hidden) detail. Finally, the front-to-front boundary is the *cm* arrangement of kinked S–As–S groups spaced with two S atoms in rows parallel to the long diagonal of the face. Thus, the *a* and *c* axes are practically identical in these sections and probability of order-disorder phenomena is very high.

Non-OD twinning

The above analysis and the fact that the 'core portions' of the As_5S_{11} groups are copies of the entire As_3S_7 groups, to which a two-As attachment is applied (see Fig. 6), bring us to realize that every time that the As_5S_{11} group is growing in a 'back-to-back' fashion on the (010) layer of As_3S_7 groups, it can stop at the As_3S_7 stage. In that case, it must be followed by a layer of As_5S_{11} groups in a 'front-to-front' relationship, *i.e.*, we observe two As_3S_7 layers 'back-to-back' together. The same happens when the thin layer in the 'back-to-back' attachment does not stop accreting and grows to become an As_5S_{11} layer, followed by the As_3S_7 layer in a 'front-to-front' orientation. Now we have a 'back-to-back' pair of As_5S_{11} layers. In the former example, the last layer of As_5S_{11} groups can grow either in the *n*(010)-related orientation to the previous As_5S_{11} layers, resulting in the *n*(010) twin law valid for the entire structure, or it can grow in a $2||[101]$ related orientation to the previous layers, resulting in the $2||[101]$ twin law.

Makovicky & Skinner (1975) quote one more twin law, $n||(1\bar{1}0)$, again based on exchange of a combined As_3S_7 and As_5S_{11} layer by a pure As_3S_7 and As_3S_7 layer, based on the 'unfinished' As_5S_{11} groups, *i.e.*, not on an OD principle. This proceeds on the $(1\bar{1}0)$ plane of the sinnerite lattice and involves the combined As_3S_7 & As_5S_{11} slabs with this orientation (easily traceable in Fig. 6). A complete analysis of twin orientations resulting from these phenomena exceeds the scope of this paper; the interested reader is referred to Makovicky & Skinner (1975).

We suggest that an undetected array of OD and non-OD defects of the kinds presented here is responsible for the deviating As–S bond-distances and displacement parameters of As and S, which were summarized above. In Figures 7 and 8 we see that, except for As3 and the S3 attached to it, both of which form part of the As_3S_7 chain, the As and S atoms in question form part of the As_5S_{11} chain. They are concentrated on its branches: As7 with a high displacement factor, As6 from the short branch of the As_5S_{11} group, which is associated with S atoms with high displacement factors, and As5 with attached S2 and S15 (for details see above). These branches are sites of enantiomorphous exchange, chain-length mistakes, and OD phenomena. Thus, we suggest that, in spite of a pure single-crystal appearance, the examined sinnerite crystal contains a portion of the above-described defects. These produce spurious contributions to the measured reflections, as well as contributions to the subcell reflections and, in turn, produce effects superimposed onto a regular structure in the process of Fourier transformations, resulting in the observed deviations from a simple, more regular structure model. The near-perfect character of the natural crystal can be tentatively ascribed to slow

TABLE 4. BOND VALENCE SUMS FOR ATOMS IN SINNERITE

	As1	As2	As3	As4	As5	As6	As7	As8	Cu1	Cu2	Cu3	Cu4	Cu5	Cu6	Cu7	Cu8	Cu9	Cu10	Cu11	Cu12	
S1						0.855				0.265	0.506	0.356									1.982
S2				0.979	1.215						0.213						0.328				2.735
S3			1.354													0.356			0.311	0.564	2.585
S4								1.215								0.328	0.397	0.244			2.184
S5	0.708						0.927								0.287			0.419			2.341
S6					1.317				0.366				0.397	0.356							2.436
S7						0.708								0.347	0.386					0.356	1.797
S8		0.953						0.832				0.320	0.231								2.336
S9	1.090													0.176			0.442		0.493		2.201
S10							1.005					0.442		0.376		0.225					2.048
S11				1.182		0.485							0.303					0.272			2.242
S12		0.810								0.231					0.408	0.303					1.752
S13			1.429										0.376		0.303		0.287				2.395
S14			0.810					1.061	0.213		0.337										2.421
S15	0.927				0.902					0.303										0.419	2.551
S16				0.855					0.442			0.328								0.311	1.936
S17		1.151									0.328							0.257	0.430		2.166
S18							0.788		0.337	0.347									0.442		1.914
	2.725	2.914	3.593	3.016	3.434	2.048	2.720	3.108	1.358	1.146	1.384	1.446	1.307	1.255	1.384	1.212	1.454	1.192	1.676	1.650	

rates of growth on the one hand and to the presumed absence of (010) as a growing face on the other hand.

Acknowledgments

The manuscript benefitted from revisions by Frantisek Laufek and one anonymous reviewer. Lee Groat and Andreas Ertl are thanked for the efficient handling of the manuscript. The research was supported by "Progetto d'Ateneo 2012, University of Firenze" to LB and by "Progetto d'Ateneo 2006, University of Padova" to FN.

References

Brese, N.E. & O'Keeffe, M. (1991) Bond-valence parameters for solids. *Acta Crystallographica* **B47**, 192–197.

Graeser, S., Cannon, R., Drechsler, E., Raber, T., & Roth, P. (2008) *Faszination Lengenbach Abbau-Forschung-Mineralien 1958–2008*. Kristallographik Verlag, Achberg, 192p.

Ibers, J.A. & Hamilton, W.C., Eds. (1974) *International Tables for X-ray Crystallography, Volume IV*. Kynoch Press, Dordrecht, The Netherlands, 366p.

Makovicky, E. & Skinner, B.J. (1972) Studies of the sulfosalts of copper. II. The crystallography and composition of sinnerite, $Cu_6As_4S_9$. *American Mineralogist* **57**, 824–834.

Makovicky, E. & Skinner, B.J. (1975) Sulfosalts of copper. IV. Structure and twinning of sinnerite, $Cu_6As_4S_9$. *American Mineralogist* **60**, 998–1012.

Marumo, F. & Nowacki, W. (1964) The crystal structure of lautite and of sinnerite, a new mineral from the Lengenbach Quarry. *Schweizer Mineralogische und Petrographische Mitteilungen* **44**, 440–454.

Maske, S. & Skinner, B.J. (1971) Studies of the sulfosalts of copper. I. Phases and phase relations in the system Cu-As-S. *Economic Geology* **66**, 901–918.

Sheldrick, G.M. (2008) A short history of SHELX. *Acta Crystallographica* **A64**, 112–122.

Received November 4, 2013, revised manuscript accepted January 10, 2014.